

Mitigation of Power Quality Event Using FACT'S Device

Harish D Mude, Purushottam R Bharambe, Ravishankar S Kankale

ABSTRACT—This paper introduces a novel method for the mitigation of the voltage sag and voltage flicker by using Kalman filter and its derivatives (adaptive, and extended). The Kalman filter is used as a tool to extract both the instantaneous envelope of the voltage sags, and to extract the Instantaneous Flicker Level (IFL) of the voltage flicker. Also, this paper demonstrates the advantages of using the Kalman filter instead of the existing tools for tracking and extracting voltage disturbances. Digital simulation results are presented to illustrate the mitigation of unbalanced voltage sags, and the compensation of the cyclic and noncyclic voltage flicker by employing the proposed algorithm.

INDEX TERMS—DSTATCOM, Kalman filter, unbalanced voltage sags, voltage flicker.

I. INTRODUCTION

IN THE deregulated power market, complying with the Power Quality (PQ) standards is becoming a major issue for the competing power distribution utilities. The revenue losses to US businesses due to poor PQ are estimated to be of 4 billions annually [1]. Voltage sag is a vital issue for system performance. Usually, voltage sags cause the malfunction of the modern process control, programmable logic control, and variable speed drives; in addition, sags can initiate significant tripping off for voltage-sensitive loads. Another critical issue is the voltage flicker, which is the most difficult PQ problem from the mitigation prospective, because of the chaotic characteristics of voltage flicker. This problem has increased in the industrial distribution systems because of the proliferation of nonlinear varying loads such as arc furnaces, arc welders, spot welders, and shredder motors [2].

Recently, the mitigation of the voltage sags has become the focus of PQ research to minimize its severe economical impact [3]. Many techniques have been introduced in the literature to track and extract voltage sags. The α - β technique has been used to extract the voltage sags, but it does not give satisfactory results for unbalanced voltage sags [4], [5]. The instantaneous power theory (pq theory) has been also utilized to extract voltage sags [6], but it requires pure sinusoidal waveforms for its voltage and current; otherwise, the results are not accurate [7]. Fast Fourier Transform (FFT) and Phase Locked Loop (PLL) have been often employed to mitigate voltage sags, but these techniques do not yield accurate results if a voltage sag is associated with a phase angle jump [8].

In addition, the adaptive perceptron has been applied to track voltage sags, and it does give satisfactory results [9]. Different topologies have been mentioned in the literature for sag mitigation. The most efficient mitigating device for voltage sags has continued to be the Dynamic Voltage Restorer (DVR), because of its fast response, simple control, and fewer transients [10]. Recently, the Distribution STATic COMPensator (DSTATCOM) has become widely adopted as an efficient mitigating device. It has the advantage of optimized energy which the DVR does not have, since the DVRs are mostly connected to the source of energy because the DVR usually injects active and reactive power to restore the load voltage [11], [12].

Voltage flicker is another PQ problem that has attracted attention recently. From the mitigation prospective, voltage flicker is the most difficult voltage challenge because of its randomness which hinders tracking. The mitigation of voltage flicker will definitely limit the effect of voltage flicker on end-line customers. Most of the existing extracting techniques for voltage flicker depend on the FFT and its derivatives [13], [14], but FFT comes with some drawbacks such as slow response, picket fence, and leakage [15]. The p-q theory can also be used as a technique for flicker extraction and it gives satisfactory results for flicker mitigation [16]–[18]. The traditional mitigating device for voltage flicker depends on the Static VAR Compensator (SVC) which plays a crucial role for mitigating flicker produced by arc furnaces [14], and [19]. However, SVC has a low control update rate (it is about half a cycle), and its limited capabilities for (Instantaneous Flicker Level) IFL mitigation [14]. As a result of the SVC's pitfalls, the DSTATCOM has come into the market as a substitute for the SVC [16], and [20]. The DSTATCOM gives a much better performance than the SVC, but is still not widely used because of its costs and the complexity of the control circuit [14].

This paper introduces a modular approach mitigating device in which the DSTATCOM is the proposed mitigating device for voltage sags and flicker voltage (the modular approach consists of three DSTATCOMs, one DSTATCOM for each phase). The privilege of the modular approach is that it is capable of mitigating voltage disturbances of each phase individually, if three-phase disturbances are uncorrelated. The proposed algorithm for voltage disturbance extraction is the Kalman Filter (KF). It is an accurate algorithm for signal tracking, and has been utilized in the power sector for disturbance extraction [21]–[23]. The proposal in this paper is that the KF and its derivatives, adaptive and extended, are used as a unified approach to extract the instantaneous unbalanced voltage sags, and the instantaneous modulating signal of voltage flicker. Consequently, voltage sags and voltage flicker can adaptively and efficiently be mitigated using only one unified mitigating device.

This paper is organized in three sections. The proposed algorithm for voltage disturbance extraction of voltage sags and voltage flicker is. These results are illustrated to prove the efficiency of the proposed control algorithm for the extraction and mitigation of the voltage sags and voltage flicker. Finally, the paper's proposal is concluded.

II. PROPOSED ALGORITHM

In this section, the KF and its derivatives are mathematically explained. The formulation of the KF to extract the instantaneous voltage envelope for voltage sags and the modulating signal for voltage flicker is presented. The first two parts of this section examine the tracking of voltage sags, and voltage flicker; the last part illustrates the generalized control block, which is adopted to operate the DSTATCOM.

A. Kalman Filter for Voltage Sags

The KF has many favorable features for tracking random and noisy signals. In this paper, the KF is formulated to track the three-phase voltages during the disturbance period to detect voltage sags, swells, and fluctuations. The phase voltage is expressed by

$$v(t) = M \times \sin(\omega_0 t + \theta_0) \tag{1}$$

where M is the magnitude of the phase voltage, ω_0 is a constant ($2\pi \times 60$), and θ_0 is the phase shift of the phase voltage. The state-space equations of the phase voltage are defined as follows

$$x'_{k+1} = A \times x'_k + B \times u_{k+1} + w_k \tag{2}$$

$$z_k = H \times x'_k + v_k \tag{3}$$

where $x'_k = [x'_{1k} \ x'_{2k}]^t$, x'_1 and x'_2 are in-phase and quadrature components of the magnitude M . $u_{k+1} = 0$, $A = \begin{bmatrix} 0 & 1 \\ 1 & 0 \end{bmatrix}$, $B = 0$, $H = [\cos(\omega_0 t_k) \ -\sin(\omega_0 t_k)]$, t_k is the time at iteration k , w_k and v_k are the uncorrelated Gaussian white noise sequence with means and covariance as follows:

$$E\{w_i\} = 0; \quad E\{w_i w_j^T\} = Q \delta_{ij}, \quad \text{for all } i, j \tag{4}$$

$$E\{v_i\} = 0; \quad E\{v_i v_j\} = R \delta_{ij}, \quad \text{for all } i, j \tag{5}$$

where; $E\{\cdot\}$ denotes the expectation, and δ_{ij} denotes the Kronecker delta function. Q and R are the covariance matrixes for process noise and measurement noise respectively.

Equations (2) and (3) follow a recursive process of the KF algorithm, which is detailed in Appendix A, to obtain the envelope of the voltage signal. The magnitude of this envelope is defined as follows:

$$M = \sqrt{x'^2_1 + x'^2_2}. \tag{6}$$

In an industrial system, the phase voltage is contaminated with varying noise and harmonics, and the assumption of constant values for Q and R is not acceptable. An adaptive KF algorithm is employed to track the time-varying model and system

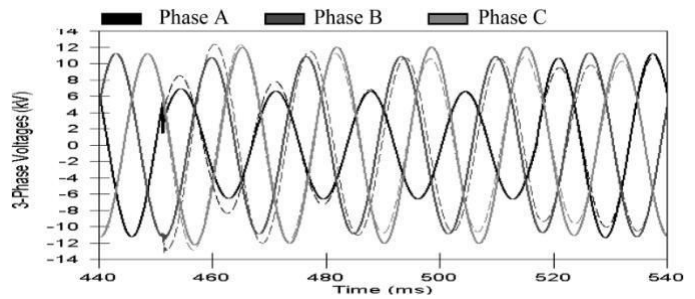


Fig. 1. d-q technique for tracking unbalanced voltage sags.

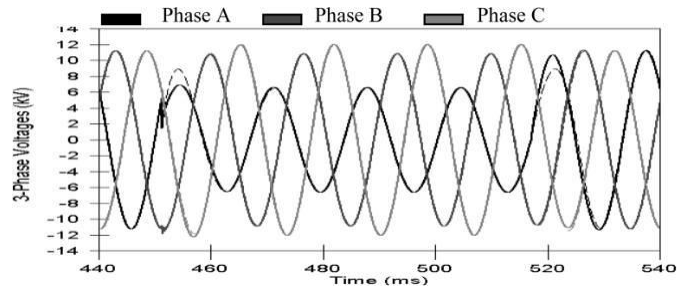


Fig. 2. Kalman filter for tracking unbalanced voltage sags.

noise through the on-line calculation of Q and R . The unbiased estimate of Q and R are obtained from the adaptive algorithm, which is given in Appendix B.

The performance of adaptive KF is compared with the $d-q$ technique to show the effectiveness of the KF for instantaneous tracking of distorted signals; $d-q$ technique is commonly used for voltage sag tracking. In the $d-q$ technique, the selection of the parameters for the Low Pass Filter (LPF) and the order of the filter play a crucial role in the filter performance. As the filter order is increased the filtration process gets improved, but the time response gets worse and the phase shift of the output signal becomes bigger. Also, the selection of the cut off frequency affects the transient response of the filter because it is related to the time constant of the filter. It is a matter of tradeoff between the harmonic rejection of the input signal, and the speed of the filter due to any transient of the input signal, ($d-q$ technique block diagram and its parameters are listed in Appendix C). Kalman filter and $d-q$ technique are applied to the pure-sinusoidal unbalanced voltage sags, and the adaptive KF for pure-sinusoidal unbalanced voltage sags are plotted in Figs. 1 and 2, respectively. Also, Figs. 3 and 4 illustrate $d-q$ technique and KF results of tracking for distorted unbalanced voltage sags, respectively. In these figures, the curves with the solid lines and dashed lines represent the original and tracked phase voltage waveforms respectively. A comparison of these figures denotes the superiority of the KF for tracking unbalanced voltage sags. Moreover, The KF shows accurate tracking of the magnitudes and angles for the three phases, also it shows the fastness of the instantaneous tracking which ranges from quarter to half a cycle. Whereas the $d-q$ technique takes at least one cycle to track the sagged voltage of the faulted phase (phase A). Also, the $d-q$

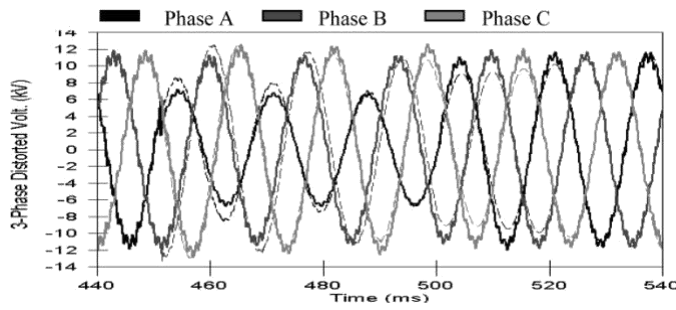


Fig. 3. d-q for tracking distorted unbalanced voltage sags.

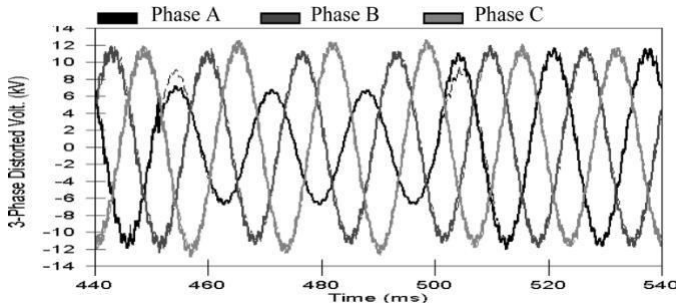


Fig. 4. Kalman filter for tracking distorted unbalanced voltage sags.

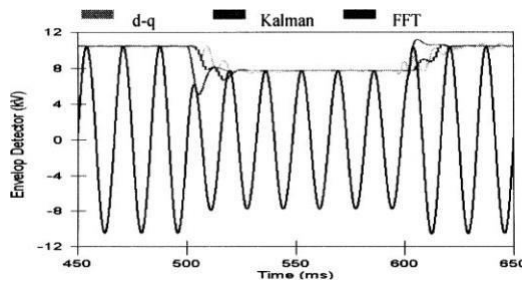


Fig. 5. Envelope detection using Kalman filter, FFT, and d-q.

technique indicates some differences in magnitudes and phase shifts in the non-faulted phases (phase B and C) as shown in Figs. 1 and 3.

The novel application of the KF in this paper is to precisely detect the envelope of the distorted waveform which is a unique feature of the KF compared to other commonly techniques.

The comparison between the KF and other techniques for detecting the instantaneous voltage envelope of the sagged voltage is shown in Fig. 5; the tracking of the voltage envelope is obtained by using the KF, d-q technique, and FFT. It is obvious from the curve that the FFT takes approximately 1 cycle to detect the magnitude; - takes about 2 cycles to detect the magnitude with a little oscillation. Whereas, the KF can detect the change in the envelope within less than half a cycle. Now the KF proves to be an excellent tool for instantaneous tracking and envelope detection for the voltage sags with respect to the other existing techniques.

B. Kalman Filter for Voltage Flickers

In the previous section, obtaining the envelope of the signal was presented. The next step to extract the modulating signal

and calculate the IFL is to formulate the magnitude of the envelope as follows:

$$M = M_0 + S_m \tag{7}$$

where M_0 is the constant peak of the fundamental voltage, and S_m is the instantaneous modulating signal, which is mathematically presented by the magnitude of the IFL.

To separate the constant component M_0 from the IFL, the following state-space equations are proposed as,

$$x_{1k+1} = \begin{bmatrix} 1 & 0 \\ 0 & 1 \end{bmatrix} x_{1k} + w_k \tag{8}$$

$$z_{1k} = [1 \ 1] x_{1k} + v_k \tag{9}$$

where

$$x_1 = [x_{11} \ x_{12}]^t$$

where x_{11} is a constant component which is M_0 and x_{12} is the IFL which can be formulated with new state variables to extract its instantaneous value, frequency, and nonsinusoidal component. Therefore, IFL can be expressed as follows:

$$IFL = x_{24} + x_{21} \times \cos(2 \times \pi \times x_{23} \times t) - x_{22} \times \sin(2 \times \pi \times x_{23} \times t) \tag{10}$$

where x_{21} is the in-phase component of the IFL, x_{22} is the quadrature component of the IFL, x_{23} is the frequency of the IFL, and x_{24} is the nonsinusoidal component.

The state-space equations, to express (10), are defined as follows:

$$\begin{bmatrix} x_{21(k+1)} \\ x_{22(k+1)} \\ x_{23(k+1)} \\ x_{24(k+1)} \end{bmatrix} = \begin{bmatrix} \cos(2\pi x_{23} \Delta t) & -\sin(2\pi x_{23} \Delta t) & 0 & 0 \\ \sin(2\pi x_{23} \Delta t) & \cos(2\pi x_{23} \Delta t) & 0 & 0 \\ 0 & 0 & 1 & 0 \\ 0 & 0 & 0 & 1 \end{bmatrix} \begin{bmatrix} x_{21k} \\ x_{22k} \\ x_{23k} \\ x_{24k} \end{bmatrix} + \begin{bmatrix} w_{21k} \\ w_{22k} \\ w_{23k} \\ w_{24k} \end{bmatrix} \tag{11}$$

$$IFL_k = (x_{21k} + jx_{22k}) \times e^{(j2\pi x_{23} \times \Delta t)} + x_{24k} \tag{12}$$

The extended KF algorithm is applied to (11) and (12), (see in Appendix E). The derivatives of the transition matrix and the KF output matrix are given in Appendix E. The magnitude of the instantaneous value for the modulating signal, (S_m), is defined as

$$S_m = \sqrt{x_{21}^2 + x_{22}^2} + x_{24} \tag{13}$$

The effectiveness of the extended KF for extracting the modulating signal is justified by comparing the KF with the FFT because the FFT is the most commonly used technique for IFL extraction. All of the in the system under study with the interface between MATLAB and PSCAD, (the FFT technique and its parameters are listed in Appendix D). The FFT and extended KF are applied to sinusoidal-modulated

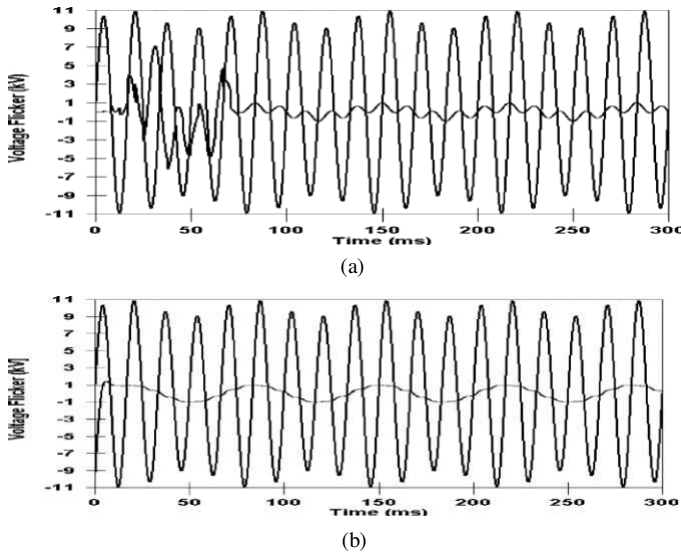


Fig. 6. (a) FFT for extraction the sin-modulated voltage flicker. (b) Kalman filter for extraction the sin-modulated voltage flicker.

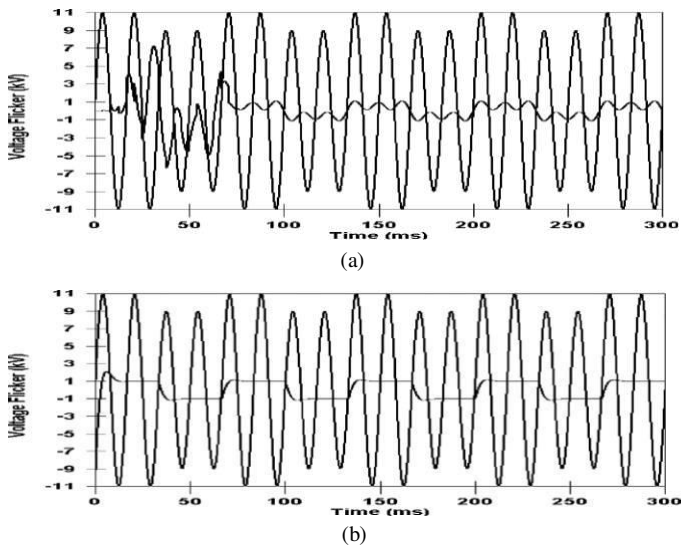


Fig. 7. (a) FFT for extraction the square-modulated voltage flicker. (b) Kalman filter for extraction the square-modulated voltage flicker.

voltage flicker as shown in Fig. 6(a) and (b), also they are applied to square-modulated voltage flicker as represented in Fig. 7(a) and (b). Each graph has the voltage flicker waveform and the extracted modulating signal S_m .

The following figures signify the capabilities of the KF for meticulously extracting the most common modulating signals for the voltage flicker. The KF is much more accurate and faster than the FFT which requires at least one cycle of its base frequency to extract the modulating signal, whereas the KF performs the about the range of frequency of the modulating signal, and it does not produce accurate results because of picket fence and leakage [14]. However, the KF does not need information about the frequency of the modulating signal. Conversely, the KF can extract the frequency of the modulating signal which is presented as a state variable of the proposed model as mentioned in (10).

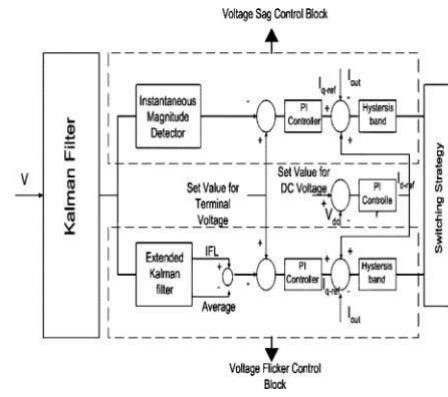


Fig. 8. Control block diagram of the proposed algorithm.

C. Proposed Control Algorithm

In the previous subsections, the results prove that the KF is an efficient tool for extracting of the disturbance signal of the voltage sags and voltage flicker. The unified control algorithm, which depends on KF, is explained in this section. The control block is illustrated in Fig. 8.

This control block consists of two main branches, the first branch is dedicated to sag mitigation, and the second branch is devoted to voltage flicker compensation. In the first branch, the adaptive KF is used to track the instantaneous voltage envelope. This process begins by obtaining the difference between the instantaneous voltage envelope and the set value. This difference is used to generate the reference signal for the quadrature component of the current, which is added to the direct component of current which flows from the DC capacitor voltage regulating loop. The resultant current is compared with the output current to operate the hysteresis current control technique. The second branch adopts the extended KF to extract S_m and average voltage value (if there is a voltage drop due to furnace currents and feeder impedance). The summation is then compared with the set value of the voltage to generate the quadrature component of the current, which is added to a similar component for the DC voltage regulation to operate the hysteresis current control technique.

III. CASE STUDY

A. System Under Study

The system configuration is exhibited Fig. 9. The DSTATCOM consists of three single-phase voltage source converters (the modular DSTATCOM) with kalman filter. The reason for such a configuration is to enable the mitigating device to restore the voltage and compensate various types of voltage flicker. The DSTATCOM is connected at the voltage level 3 phase 415 V, 50 Hz. at the Point of Common Coupling, (PCC), of the distribution system as shown in Fig. 9.

B. Simulation Results

This section shows the outcome of the proposed algorithm and the output of the mitigation process. This section is divided into two parts; the first part demonstrates the voltage sag mitigation due to a remote single line fault, and the second

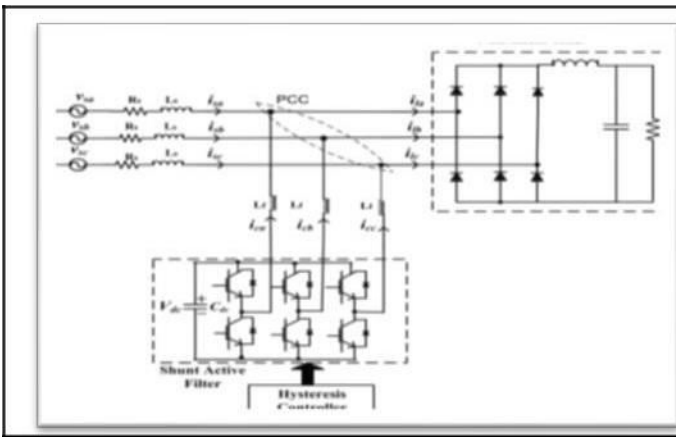


Fig. 9. Configuration of the system under study.

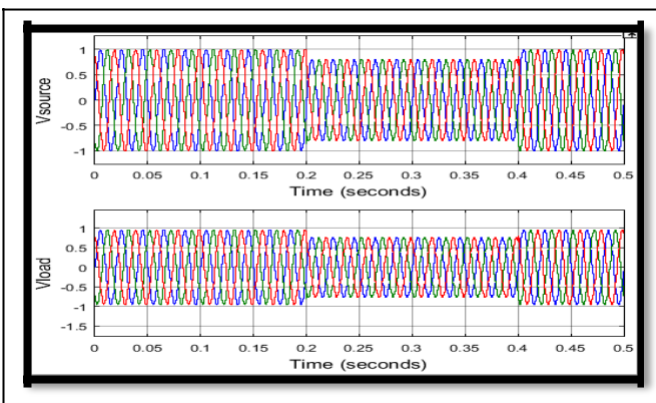


Fig. 10. Voltage of source and load without D-Statcom during voltage sag

part shows the compensation of the voltage flicker

The DSTATCOM has widely adopted as an efficient mitigating device. It has the advantage of optimized energy which the DVR does not have, since the DVR are mostly connected to the source of energy because the DVR usually injects active and reactive power to restore the load voltage. As observed above in Fig. 10, in 0.5 sec simulation, a voltage sag is introduced between 0.2 and 0.4 sec on the source side. The same has occurred on the load voltages also as there is no DSTATCOM connected. The below is the THD of the source current without DSTATCOM

The simulation results show that the voltage sags can be mitigated by inserting D-STATCOM to the distribution system. By Kalman filter to D-STATCOM, the THD is reduced within the IEEE STD 519-1992. The power factors also increase close to unity. Thus, it can be concluded that by adding D-STATCOM Kalman filter, the power quality is improved. The source current THD without D-STATCOM is recorded at 24.24%, which is considered to be very high as per IEEE standard shown in Fig. 15. The above test system is updated with D-STATCOM controlled by Kalman filter controller and the results are recorded.

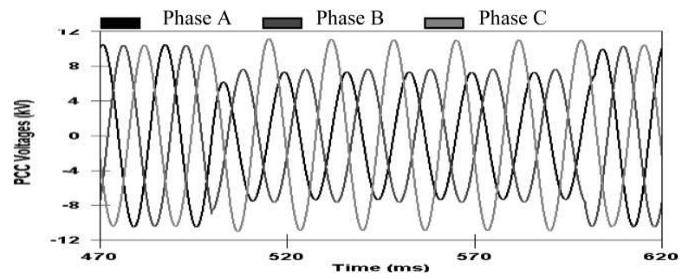


Fig. 12. Terminal voltages during the fault period.

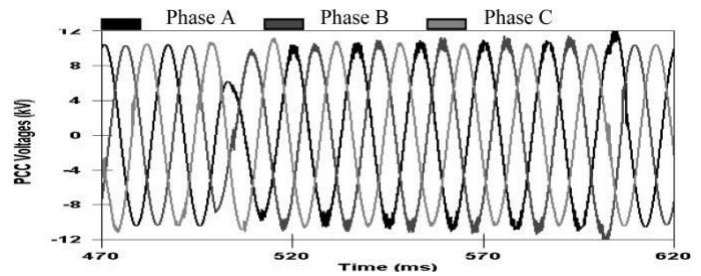


Fig. 13. Mitigation of the voltage sag, and swell during the fault period.

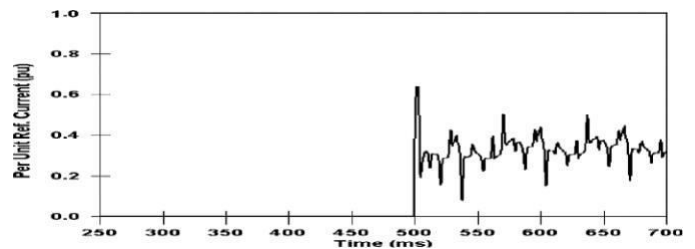


Fig. 14. Per unit current control signal.

Fig. 16 shows the source voltage has sags but the load voltage has no sag from 0.2 to 0.4 sec. As the DSTATCOM supports the load bus and the fault is mitigated. The below is the THD of the source current with DSTATCOM

Fig. 17. Shows the THD is 2.13% of the source current with DSTATCOM connected to the grid at PCC, which is maintained below 5%. The source currents, load currents, and compensation currents with D-STATCOM are recorded for the same simulation time of 0.5 sec and are shown below. The circuit is also run for voltage fluctuations in the source voltages and the graphs are recorded and are shown below. This graph belongs to the compensation of source current, load currents during the sag. A change in RMS value we called as sag, in the first graph, there is no involvement of sag, which can be easily explained from 0.2 to 0.4 sec in figure number 20

The source currents may be non-cyclic flickers and cyclic flickers; the actual output current is demonstrated in the figure above. The injected reactive power is changed. Here, the voltage oscillation is reduced from an average value of 0.005 to approximately 0.015. The significance of the reduction is indicated by the short-term flicker severity (P_{st}) as expressed

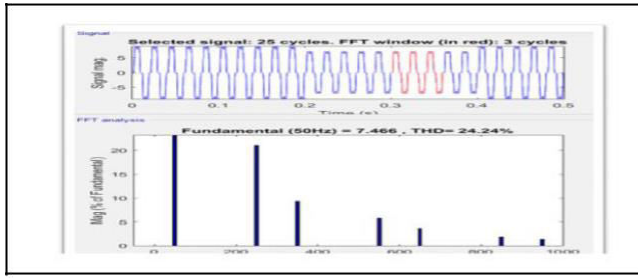


Fig. 15. FFT analysis of source current for THD calculation

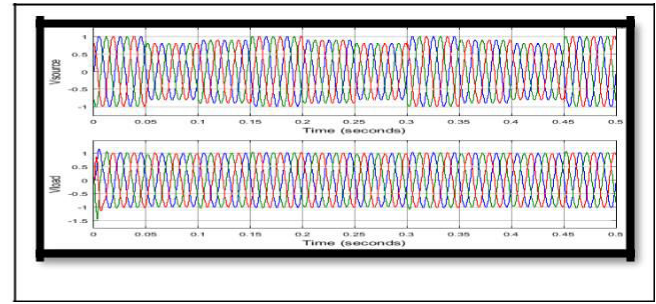


Fig. 19. Source and load voltage with D-statcom during voltage flickers

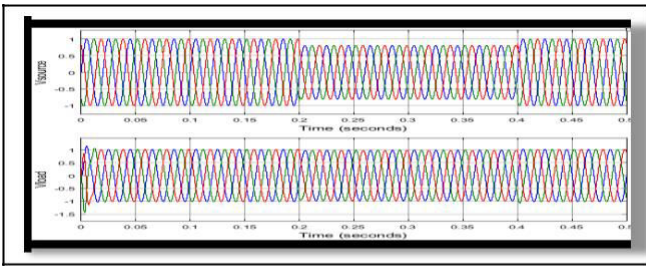


Fig. 16. Source and load voltage with D-Statcom during voltage sag

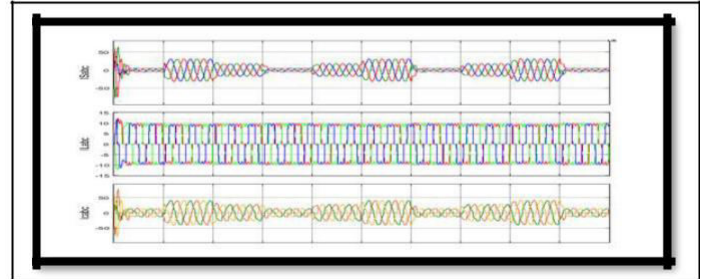


Fig. 20. Source, load and compensation (Dstatcom) current during voltage flickers

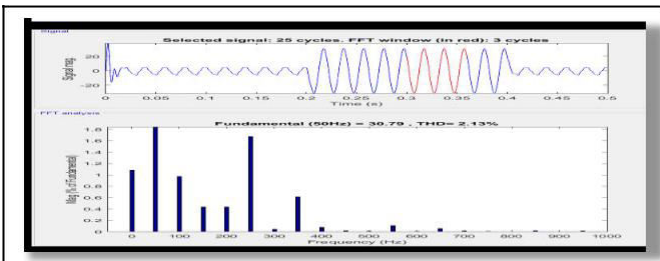


Fig. 17. FFT analysis of source current with D-Statcom during voltage sag

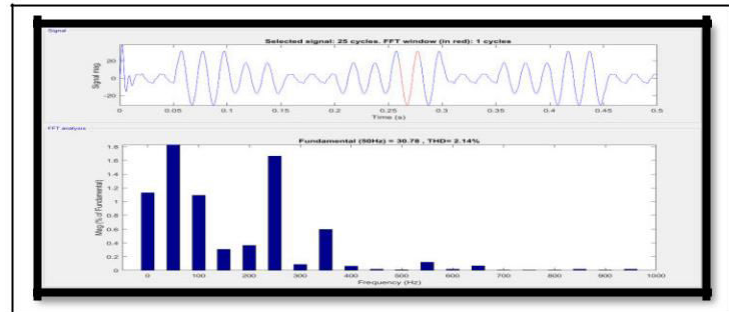


Fig. 21. FFT analysis of source current with Dstatcom during voltage flickers

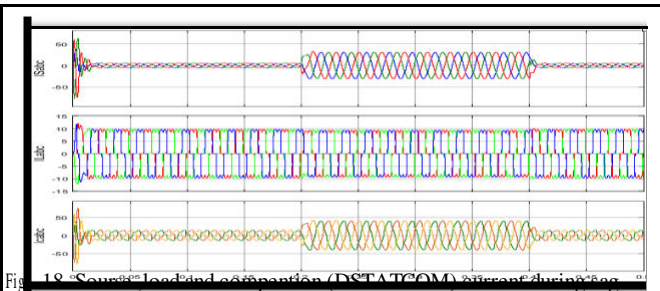


Fig. 18. Source, load and compensation (DSTATCOM) current during sag

IV. CONCLUSIONS

This paper introduces a unified mitigating device for voltage sags and voltage flicker. The proposed modular DSTATCOM mitigates voltage sags and voltage flicker, even if the voltage disturbances are unbalanced. The proposed mitigating strategy, which depends on KF, is fast and accurate for the tracking and extraction of the voltage cycle. Now the KF proves to be an excellent tool for

mitigated. Different levels of voltage sags and a voltage swell are restored simultaneously. Also, the cyclic voltage flicker is compensated efficiently and the IFL is reduced by approximately 60% of its value before the compensation.

Consequently, voltage flicker which drives from an arc furnace in its both cycles is transferred from the irritation region to lower than the observable region, based on IEEE 141-1993, and does not harm the other customers

for detecting the instantaneous voltage envelope of the sagged voltage is shown in Fig. above. The tracking of the voltage envelope is obtained by using the KF, d-q technique, and FFT. It is obvious from the curve that the FFT takes approximately 1 cycle to detect the magnitude; d-q takes about 2 cycles to detect the magnitude with a little oscillation. Whereas, the KF can detect the change in the envelope within less than half a

APPENDIX I
LINEAR KALMAN FILTER ALGORITHM

1) Time update stage:

a) Project the state ahead

$$x_k^- = A \times x_{k-1} + B \times u. \tag{15}$$

b) Project the error covariance ahead

$$P_k^- = A \times P_{k-1} \times A^T + Q. \tag{16}$$

2) Measurement update stage:

a) Compute the Kalman gain

$$K_k = P_k^- \times H^T (H \times P_k^- \times H^T + R)^{-1}. \tag{17}$$

b) Update estimate with measurement Z_k

$$x_k = x_k^- + K_k \times (z_k - H \times x_k^-). \tag{18}$$

c) Update the error covariance

$$P_k = I - K_k \times H^T \times P_k^-. \tag{19}$$

APPENDIX II

ADAPTIVE KALMAN FILTER ALGORITHM FOR ON-LINE
CALCULATION OF R AND Q

$$r_j = z_k - H \times x_k$$

where, r_j is the observation noise sample.

$$\hat{r} = \frac{1}{N} \sum_{j=1}^N r_j \tag{20}$$

where \hat{r} is sample mean for N sample.

The estimate foris obtained by first constructing an estimate for C_r , the covariance of C_r as follows

$$\hat{C}_r = \frac{1}{N-1} \sum_{j=1}^N (r_j - \hat{r}) \times (r_j - \hat{r})^T.$$

The expected value of this quantity is

$$E(\hat{C}_r) = \frac{1}{N} \sum_{j=1}^N H_j \times P_j \times H_j^T + R. \tag{23}$$

Apparently, an unbiased estimate of R is given by

$$\hat{R} = \frac{1}{N-1} \sum_{j=1}^N \left\{ (r_j - \hat{r}) \times (r_j - \hat{r})^T - \left(\frac{N-1}{N} \right) H_j \times P_j \times H_j^T \right\}. \tag{24}$$

Q has the similar algorithm.

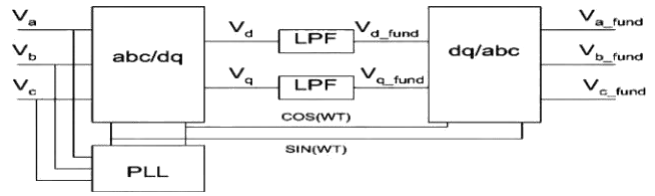


Fig. 22. d-q block diagram.

APPENDIX III

D-Q Transformation Matrix

$$\begin{bmatrix} V_d \\ V_q \\ V_0 \end{bmatrix} = \sqrt{\frac{2}{3}} \begin{bmatrix} \cos(\omega t) & \sin(\omega t) & \frac{1}{\sqrt{2}} \\ \cos(\omega t - \frac{2\pi}{3}) & \sin(\omega t - \frac{2\pi}{3}) & \frac{1}{\sqrt{2}} \\ \cos(\omega t + \frac{2\pi}{3}) & \sin(\omega t + \frac{2\pi}{3}) & \frac{1}{\sqrt{2}} \end{bmatrix} \times \begin{bmatrix} V_a \\ V_b \\ V_c \end{bmatrix} \tag{25}$$

The block diagram of the d - q technique is shown in Fig. 22.

The LPF data is:

- LPF type is butterworth filter.
- LPF has the order of 2.
- LPF cut off frequency =20Hz for d and q axes.

APPENDIX IV

FFT TECHNIQUE APPLIED FOR VOLTAGE FLICKER

The FFT is capable of extracting the modulating signal of the voltage flicker if the modulating signal frequency is known. The

(20)voltage flicker (vf) can be defined by many formulas, one of these formulas is expressed as follows:

$$vf = a_0 \times \sin(\omega_0 t + \theta_0) \times \left(1 + \sum_{n=1}^{\infty} a_{mn} \times \sin(\omega_{mn} t + \theta_{mn}) \right) \tag{26}$$

where a_0 and a_{mn} represent the required rated voltage at PCC, (should be known), and Fourier series of the modulating signal in percent respectively. θ_0 and θ_{mn} represent the required phase shift of the rated voltage at PCC, (should be known), and Fourier series phase shift of the modulating signal, respectively ω_0 and ω_{mn} represent angular frequency for the rated voltage and modulating signal respectively.

After some mathematical manipulation, the vf can be simplified as follows:

$$vf = a_0 \times \sin(\omega_0 t + \theta_0) + \sum_{n=1}^{\infty} \frac{a_0 a_{mn}}{2} \times \begin{bmatrix} \cos((\omega_0 t - \omega_{mn} t) + (\theta_0 - \theta_{mn})) \\ -\cos((\omega_0 t + \omega_{mn} t) + (\theta_0 + \theta_{mn})) \end{bmatrix}. \tag{27}$$

The 2nd and 3rd terms of (27), cos terms, can be extracted using FFT to get the Fourier coefficients of the modulating signal.

For Fig. 6(a):

The modulating signal is expressed by:

$$S_m = 0.1 \times \sin(2 \times \pi i \times 15 \times t).$$

$$\text{FFT} = 15 \text{ Hz}$$

Base frequency for

For Fig. 7(a):

The modulating signal is a square signal.

Modulating signal amplitude = 15 Hz

Modulating signal frequency = 50%

Modulating signal duty ratio = 15 Hz

Base frequency for

The modulating signal is expressed by 5 terms of the Fourier series.

APPENDIX V

EXTENDED KALMAN FILTER ALGORITHM

1) Time update stage:

a) Project the state ahead

$$x_k = f(x_{k-1}, u_k)$$

(29)

b) Project the error covariance ahead

$$P_k = A \times P_{k-1} \times A^T + Q$$

(30)

2) Measurement update stage:

a) Compute the Kalman gain

$$K_k = P_k * H^T * (H * P_k * H^T + R)^{-1}$$

(31)

b) Update estimate with measurement Z_k

$$x_k = x_k + K_k * (z_k - H * x_k)$$

(32)

c) Update the error covariance

$$P_k = (I - K_k * H) * P_k$$

(33)

A

where is defined as

$$A_{[i,j]} = \frac{\partial f[i]}{\partial x[j]}(x_k, u_k)$$

A

for the presented case is expressed as

$$A = \begin{bmatrix} \cos(2\pi x_{23} * \Delta t) & -\sin(2\pi x_{23} * \Delta t) & a_{13} & 0 \\ \sin(2\pi x_{23} * \Delta t) & \cos(2\pi x_{23} * \Delta t) & a_{23} & 0 \\ 0 & 0 & 1 & 0 \\ 0 & 0 & 0 & 1 \end{bmatrix}$$

$$a_{13} = (2\pi \Delta t) \times (-x_{21} \times \sin(2\pi x_{23} \times \Delta t) - x_{22} \times \cos(2\pi x_{23} \times \Delta t))$$

$$a_{32} = (2\pi \Delta t) (x_{21} \times \cos(2\pi x_{23} \times \Delta t) - x_{22} \times \sin(2\pi x_{23} \times \Delta t))$$

$$H_{[i,j]} = \frac{\partial h[i]}{\partial x[j]}(x_k)$$

and for paper's case the is defined as

H

$$H = [\cos(2\pi x_{23} \times \Delta t) \times \sin(2\pi x_{23} \times \Delta t) \times 2\pi \Delta t (-x_{21} \times \sin(2\pi x_{23} \times \Delta t) + x_{22} \times \cos(2\pi x_{23} \times \Delta t))1]$$

(37)

REFERENCES

- [1] M. Takeda, K. Ikeda, A. Teramoto, and T. Aritsuka, "Harmonic current and reactive power compensation with an active filter," in Proc. Power Electronic Specialist Conference, 1988, pp. 1174-1179.
- [2] T. Larsson and C. Poumarede, "STATCOM, an efficient means for flicker mitigation," in IEEE Power Engineering Society 1999 Winter Meeting, vol. 2, Jan.-Feb. 31-4, 1999, pp. 1075-1077.
- [3] M. Aredes, K. Heumann, and E. H. Watanabe, "An universal active power line conditioner," IEEE Trans. Power Del., vol. 13, no. 2, pp. 545-551, Apr. 1998..
- [4] P. Wang, N. Jenkins, and M. H. J. Bollen, "Experimental investigation of voltage sag mitigation by an advanced static VAR compensator," IEEE Trans. Power Del., vol. 13, no. 4, pp. 1461-1467, Oct. 1998
- [5] S. S. Chio, B. H. Li, and D. M. Vilathgamuwa, "Design and analysis of the inverter-side filter used in the dynamic voltage restorer," IEEE Trans. Power Del., vol. 17, pp. 857-846, July 2002.
- [6] Girgis and E. B. Makram, "Measurement of voltage flicker magnitude and frequency using a kalman filtering based approach," in Proc. Canad. Conf. Electrical and Computer Engineering, 1996, pp. 659 - 662.
- [7] Srinivasan, "Digital measurement of voltage flicker," IEEE Trans. Power Del., vol. 6, no. 4, pp. 1593-1598, Oct. 1991.
- [8] G. F. Reed, M. Takeda, F. Ojima, A. P. Sidell, R. E. Chervus, and C. K. Nebecker, "Application of a 5 MVA, 4.16 kV D-STATCOM system for voltage flicker compensation at seattle iron & metals," in Proc. of Power Engineering Society Summer Meeting, 2000, pp. 1605-1611.
- [9] S. Chen and G. Joos, "Direct power control of DSTATCOMs for voltage flicker mitigation," in Proc. Applied Power Electronics Conf., 2001, pp. 2683-2690
- [10] S. S. Chio, B. H. Li, and D. M. Vilathgamuwa, "Design and analysis of the inverter-side filter used in the dynamic voltage restorer," IEEE Trans. Power Del., vol. 17, pp. 857-846, July 2002.
- [11] H. Ma and A. A. Girgis, "Identification and tracking of harmonic sources in a power system using a kalman filter," IEEE Trans. Power Del., vol. 11, no. 3, pp. 1659-1665, Jul. 1996.
- [12] T. Larsson and C. Poumarede, "STATCOM, an efficient means for flicker mitigation," in IEEE Power Engineering Society 1999 Winter Meeting VOLOUM I
- [13] K. Srinivasan, "Digital measurement of voltage flicker," IEEE Trans. Power Del., vol. 6, no. 4, pp. 1593-1598, Oct. 1991.
- [14] A. Garcia-Cerrada, P. Garcia-Garcia-Gonzalez, R. Collants, T. Gomez, and J. Anzola, "Comparison of thyristor-controlled reactors and voltage-source inverters for compensation of flicker caused by arc furnace," IEEE Trans. Power Del., vol. 15, pp. 1225-1231, Oct. 2000.
- [15] A. A. Girgis and F. Ham, "A quantitative study of pitfalls in FFT," IEEE Trans. Aerospace Electron. Syst., vol. 16, no. 4, pp. 434-439, Jul. 1980.
- [16] G. F. Reed, M. Takeda, F. Ojima, A. P. Sidell, R. E. Chervus, and C. K. Nebecker, "Application of a 5 MVA, 4.16 kV D-STATCOM system for voltage flicker compensation at seattle iron & metals," in Proc. of Power Engineering Society Summer Meeting, 2000, pp. 1605-1611.
- [17] S. Chen and G. Joos, "Direct power control of DSTATCOMs for voltage flicker mitigation," in Proc. Applied Power Electronics Conf., 2001, pp. 2683-2690.

- (36) nace supply system by an active capacitor—A novel voltage stabilizer in power systems,” *IEEE Trans. Ind. Appl.*, vol. 31, no. 1, pp. 107–111, Jan./Feb. 1995.
- [19] M. Z. El-Sadek, M. Dessouky, and G. A. Mahmoud, “A flexible AC transmission system (FACTS) for balancing arc furnace loads,” *Electric Power System Research*, pp. 211–217, 1997.



[20